Highly Efficient and Sustained Electrochemical Hydrogen Evolution by Embedded Pd-Nanoparticles on a Coordination Polymer - Reduced Graphene Oxide Composite
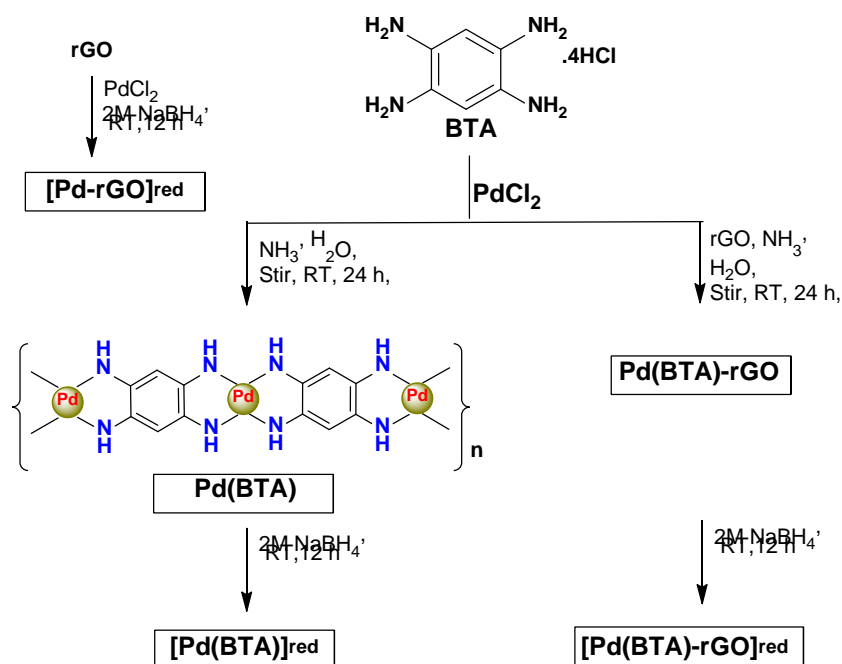
Chandraraj Alex[a,b], Sachin A. Bhat[a,b], Neena S. John[a,*] and C. V. Yelamaggad[a,*]

[a]*Centre for Nano and Soft Matter Sciences (CeNS), Jalahalli, Bengaluru 560 013, India.*
[b]*Department of Chemistry, Mangalore University, Mangalagangotri 574 199, India*
* Corresponding Authors: E-mails - jsneena@cens.res.in; yelamaggad@cens.res.in

Supporting information

Scheme

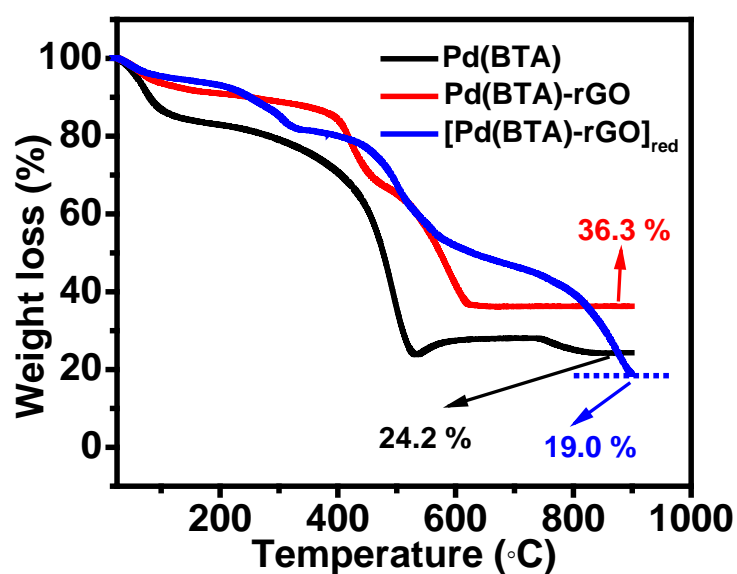**Figure S1.** Synthesis of materials investigated for HER

Figure S2. TGA curves collected in an oxygen atmosphere for the materials **Pd(BTA)** (black trace), **Pd(BTA)-rGO** (red trace)and **[Pd(BTA)-rGO]**ᵣₑ𝒹 (blue trace).
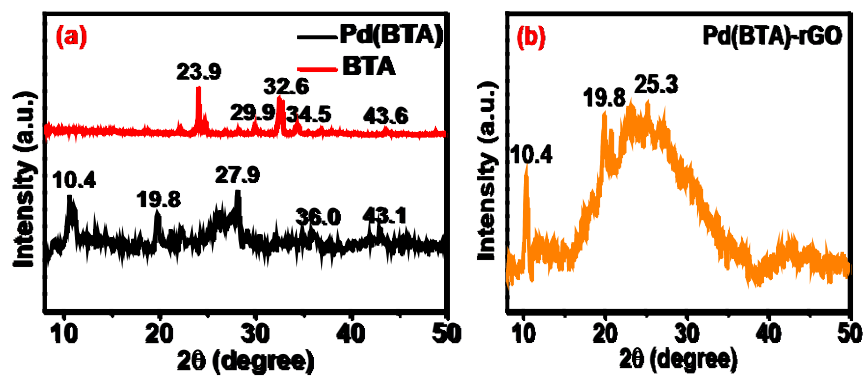

Figure S3. XRD of pristine (a) **BTA** and **Pd(BTA)** (b) **Pd(BTA)-rGO**
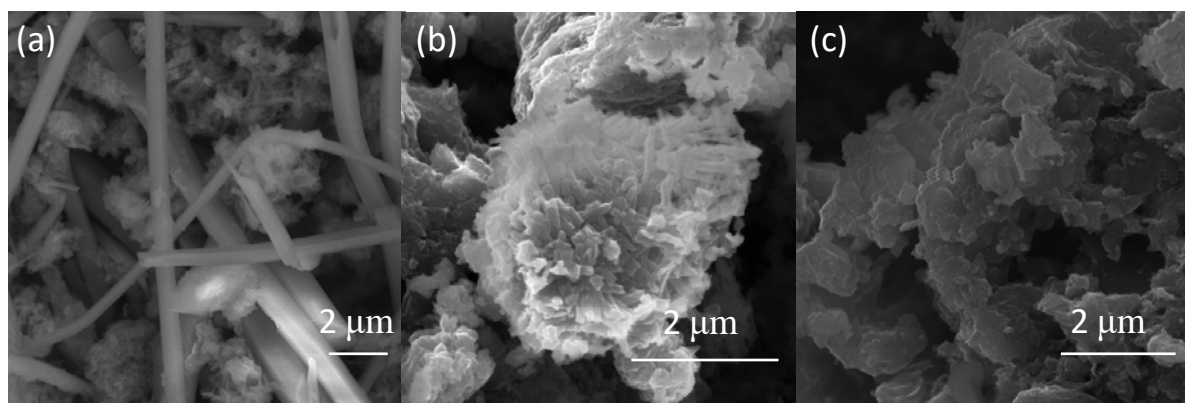
Figure S4. FE-SEM images of (a) **Pd(BTA)** (b) **Pd(BTA)-rGO** and (c) **[Pd(BTA)-rGO]**$_{red}$
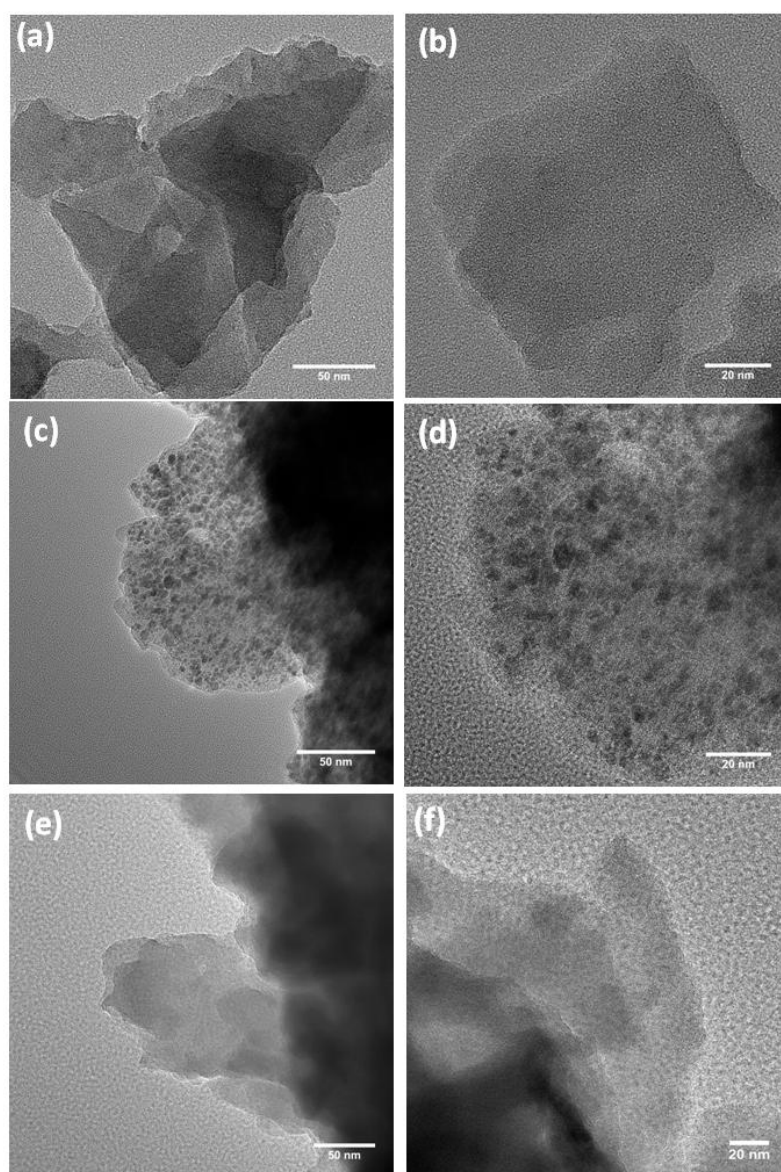

Figure S5. TEM images of (a,b)**Pd(BTA)** , (c,d) **[Pd(BTA)]**$_{red}$ and (e,f) **Pd(BTA)-rGO**.
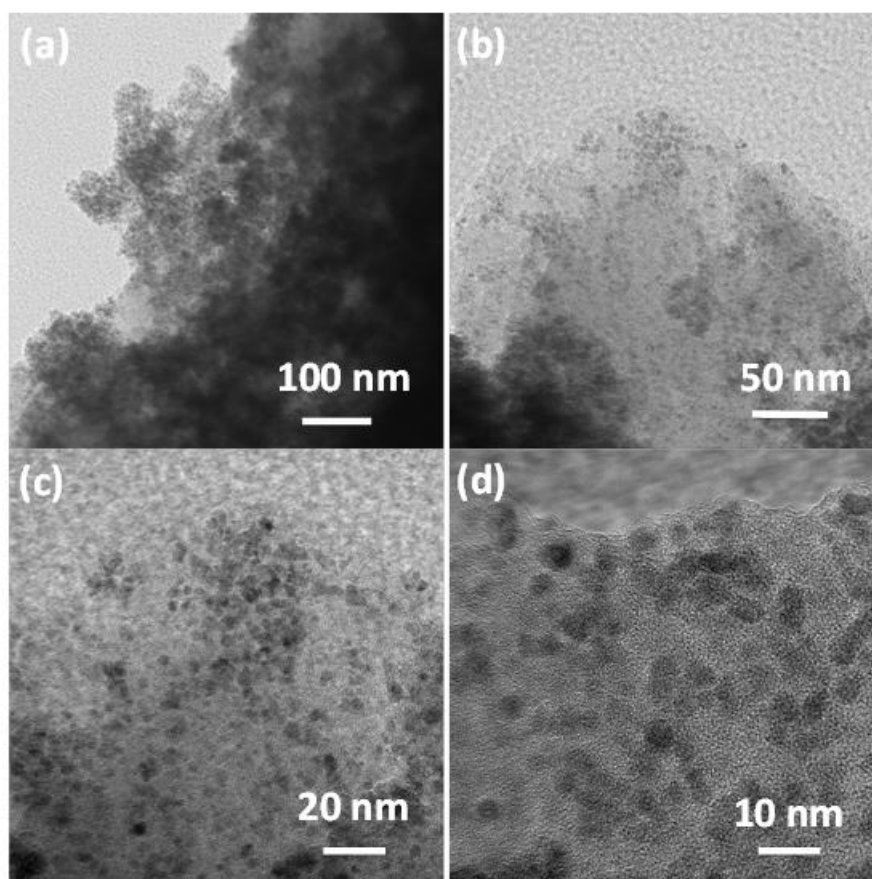
Figure S6. TEM images of **[Pd(BTA)-rGO]red** at different magnifications (a-d) lower to higher magnification
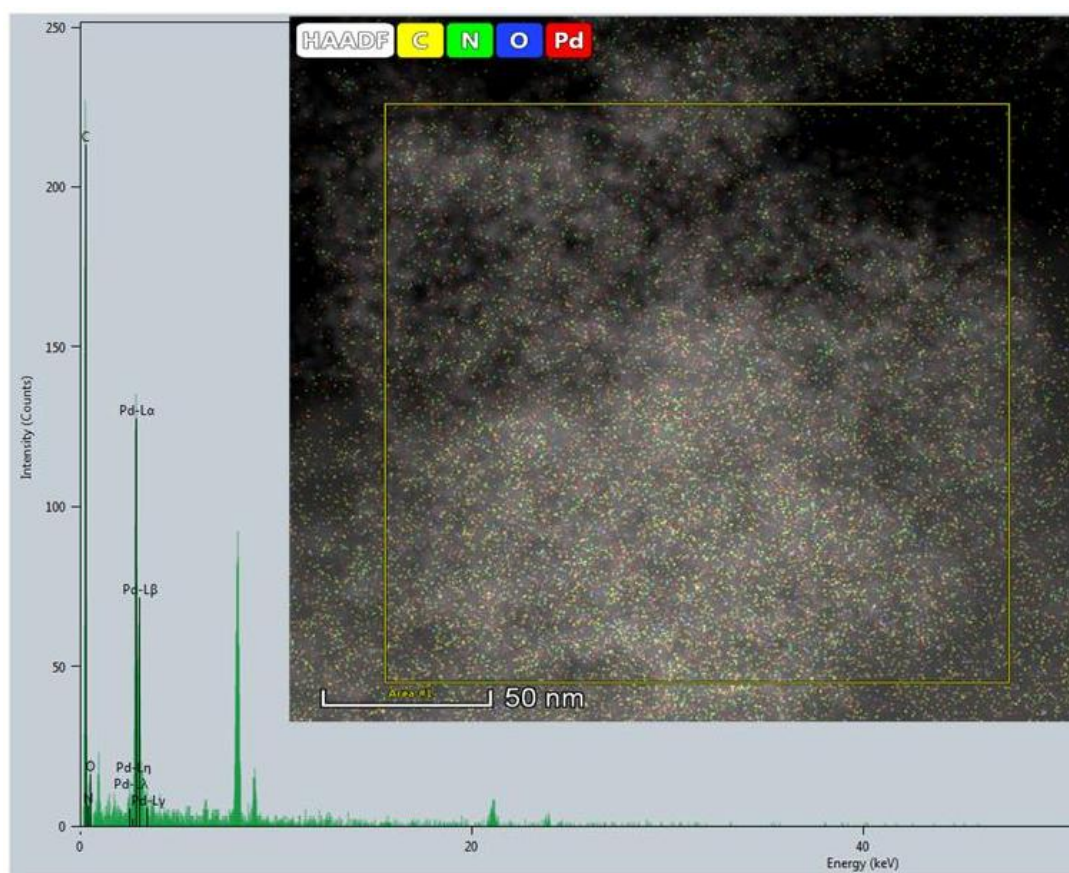
Figure S7. EDS spectra of **[Pd(BTA)-rGO]red**; the inset (yellow square) shows the area scanned for EDS acquisition

Table S1. Atomic percentage of various elements in **[Pd(BTA)-rGO]red** sample derived from the EDS spectra

Z	Element	Family	Atomic Fraction (%)	Atomic Error (%)	Mass Fraction (%)	Mass Error (%)	Fit error (%)
6	C	K	75.96	5.15	46.71	2.79	2.36
7	N	K	10.17	2.14	7.14	1.49	2.07
8	O	K	5	1.31	4.17	1.09	15.81
46	Pd	K	8.86	1.21	41.97	5.58	0.91

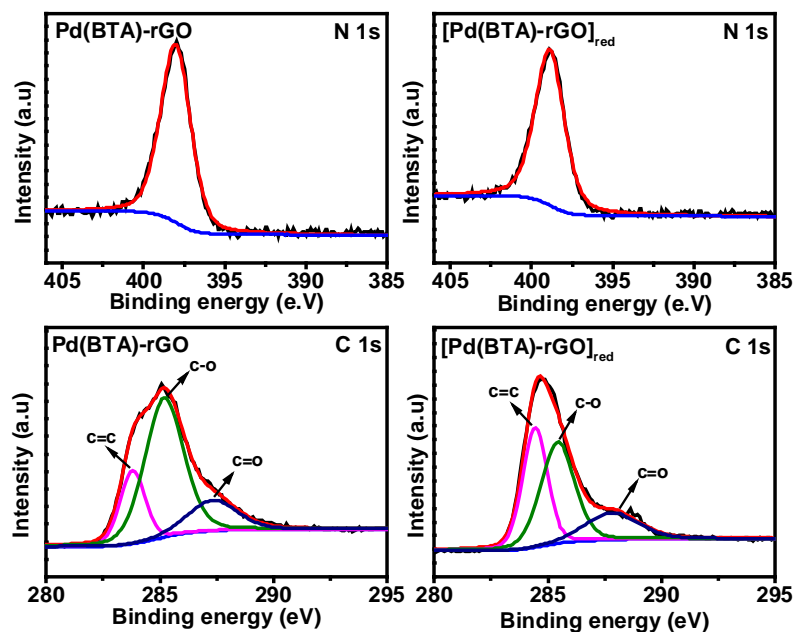**Figure S8.** XPS profiles of the samples **Pd(BTA)-rGO** and **[Pd(BTA)-rGO]red**; N 1s (top) and C 1s (bottom).
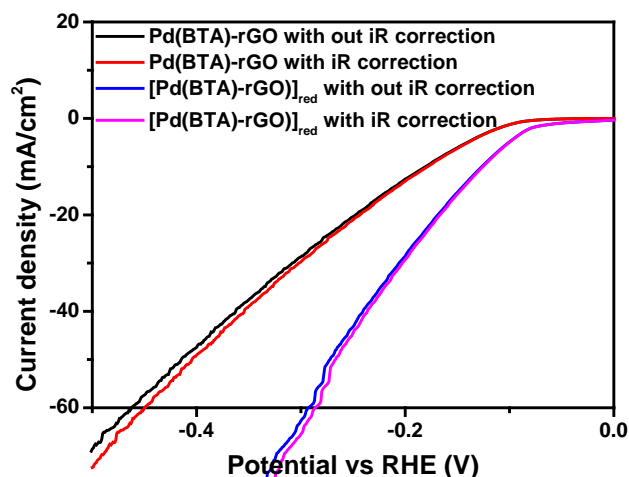
Figure S9. LSV of **Pd(BTA)-rGO** and **[Pd(BTA)-rGO]red** with and without iR compensation.

S10: TOF Calculation

Number of active sites (n) has calculated by using the formula,

n = Area under the CV curve / $2F$

Area under the curve of Pd(BTA)-rGO and [Pd(BTA)-rGO]red is calculated by integration of CV given in Figure S14a

$$A_{Pd(BTA)\text{-}rGO} = 1.99218 \times 10^{-4}$$

$$A_{[Pd(BTA)\text{-}rGO]red} = 4.17881 \times 10^{-4}$$

$$n_{Pd(BTA)\text{-}rGO} = 1.03222 \times 10^{-9}$$

$$n_{[Pd(BTA)\text{-}rGO]red} = 2.16519 \times 10^{-9}$$

TOF calculated by using the formula,

$$TOF = I / 2nF$$

I = current observed from linear sweep voltammetry at -0.2 V vs RHE (A)
n = number of active sites (moles)

F = Faraday constant (coulombs /mole).

The value ½ has included because two electrons are required to generate one H_2 molecule

$(2H^+ + 2e = H_2)$.

TOF of Pd(BTA)-rGO = 65.8 s^{-1} @ -0.2 V vs RHE.

TOF of [Pd(BTA)-rGO]$_{red}$ = 68.7 s^{-1} @ -0.2 V vs RHE.

S11. Faradaic efficiency Calculation

The Faradaic efficiency calculation of catalyst [Pd(BTA)rGO]red has carried out by constant potential chronoamperometric study. The constant potential of -0.78 V vs RHE was maintained for 1 hour and the gas was collected by inverse burette method. The Pd(BTA)-rGO]$_{red}$ produces 82 mL of gas in the 1 hour time period and we are able to get around 88.1 % Faradaic efficiency.

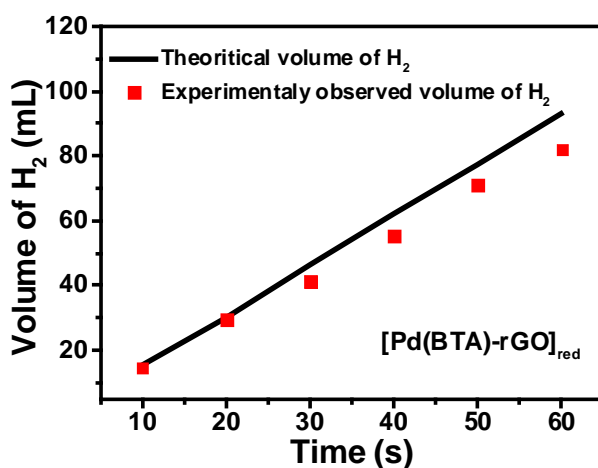**Figure S11**. The plot represent amount of H_2 collection with time during HER for **[Pd(BTA)-rGO]$_{red}$**

The amount of gas evolved during the HER reaction calculated by using faraday first law of electrolysis with the following equation.

Mole of H_2 = ½ $\int_0^t I.\,dt\ /F$

I = observed current during reaction (A); t = time of electrolysis (s); F = Faraday constant (96485 C/mol).
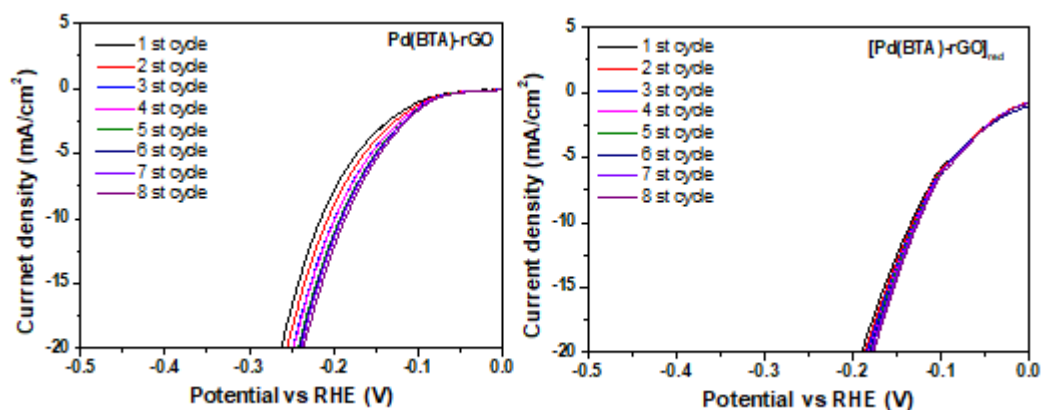
Figure S12. LSV of **Pd(BTA)-rGO** and **[Pd(BTA)-rGO]red** for different number of cycles.

Table S2. Values of various HER parameters from repetitive LSV cycles.

No. of cycles	Pd(BTA)-rGO			[Pd(BTA)-rGO]red		
	$(-)\,\eta_{10}$ (mV)	Tafel slope (mV/dec)	TOF (s^{-1}) @ -0.2 V	$(-)\,\eta_{10}$ (mV)	Tafel slope (mV/dec)	TOF (s^{-1}) @ -0.2 V
1.	215	76	39.6	133	60	53.1
2.	207	73	44.9	131	59	55.2
3.	199	70	51.4	129	59	56.7
4.	198	69	51.7	128	58	58.5
5.	192	67	56.4	128	58	58.5
6.	191	66	57.2	127	61	58.8
7.	189	65	58.8	126	59	60.5
8.	186	64	60.8	125	60	62.3
Average	**197.125**	**68.750**	**52.6**	**128.375**	**59.25**	**57.95**
S^2	**96.41**	**17.071**	**53.11**	**6.83**	**1.07**	**8.47**
S.D	**9.8**	**4.1**	**7.28**	**2.61**	**1.03**	**2.91**

S^2 = Sample variance.

S.D = Standard deviation.

Formula for calculation of standard deviation (SD):

$$S^2 \quad = \sum (x_i - x_{mean})^2 / (n-1).$$

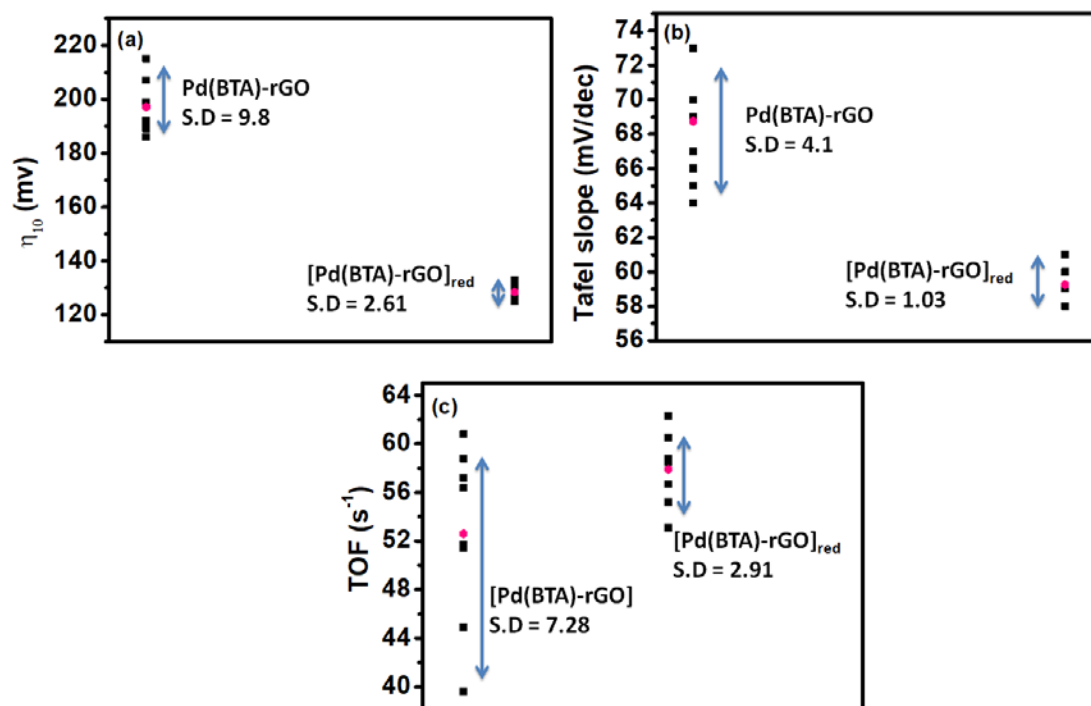$$X_{mean} = \sum x_i / n.$$

$$S.D = \sqrt{sample\ variance}$$

Figure S13. (a) (b) and (c) represent standard deviation plot of **Pd(BTA)-rGO and [Pd(BTA)-rGO]red** for various HER parameters.
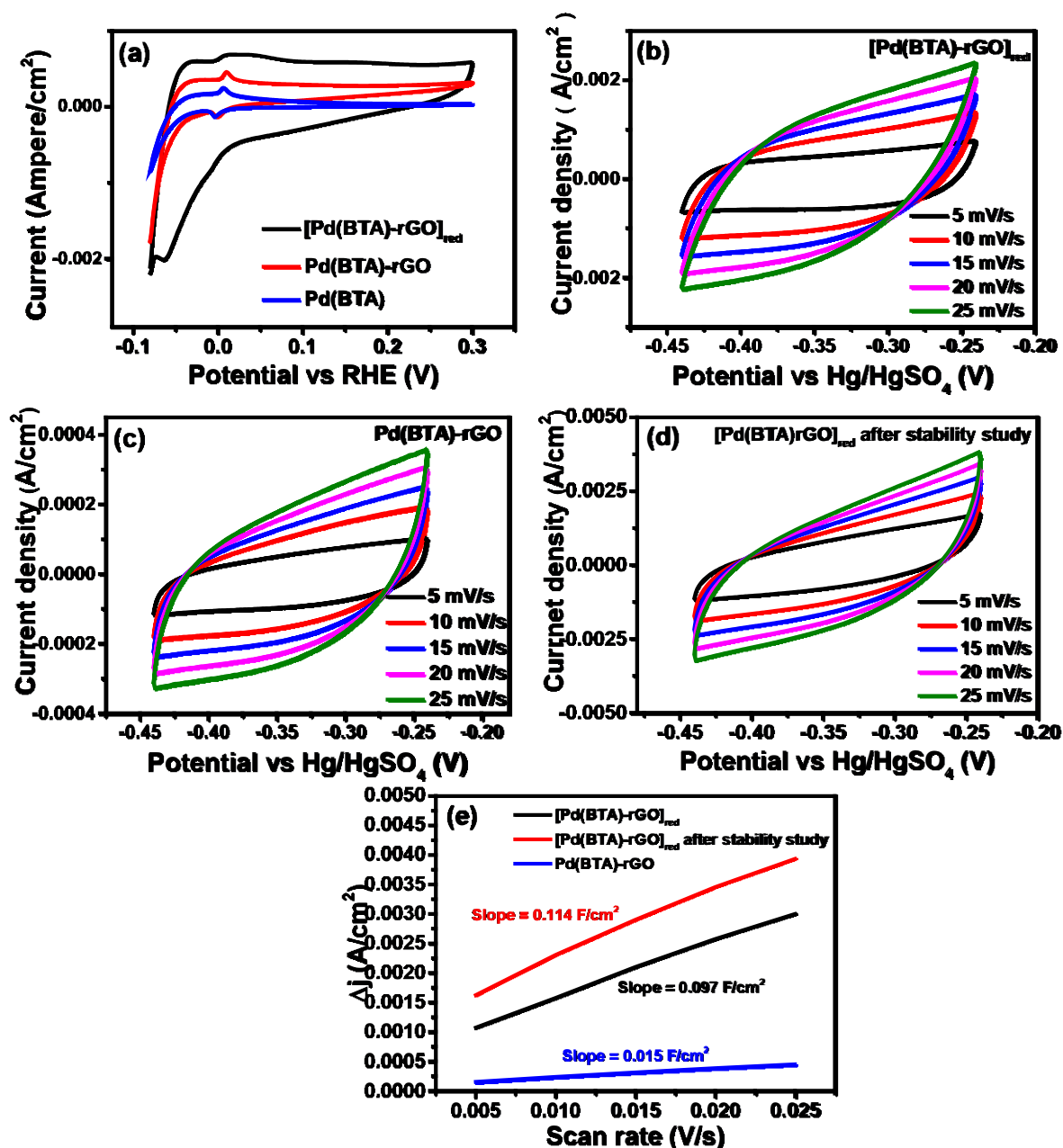
Figure S14. (a) Cyclic voltammograms recorded at a scan rate of 10 mV/s for the samples **Pd(BTA)** (blue-trace), **Pd(BTA)-rGO** (red-trace) and **[Pd(BTA)-rGO]red** (black-trace); (b) and (c) Cyclic voltammograms of **[Pd(BTA)-rGO]red** and **Pd(BTA)-rGO** at different scan rates (d) Cyclic voltammograms of **[Pd(BTA)-rGO]red after stability test** at different scan rates; (e) ECSA value of **[Pd(BTA)-rGO]red** (black trace), **[Pd(BTA)-rGO]red after stability study** (red trace), **Pd(BTA)-rGO** (blue-trace) obtained at -0.34 V.

Figure S15. (a) Equivalent circuit model and (b) corresponding fitted diagram of the equivalent circuit for **[Pd(BTA)-rGO]red** .
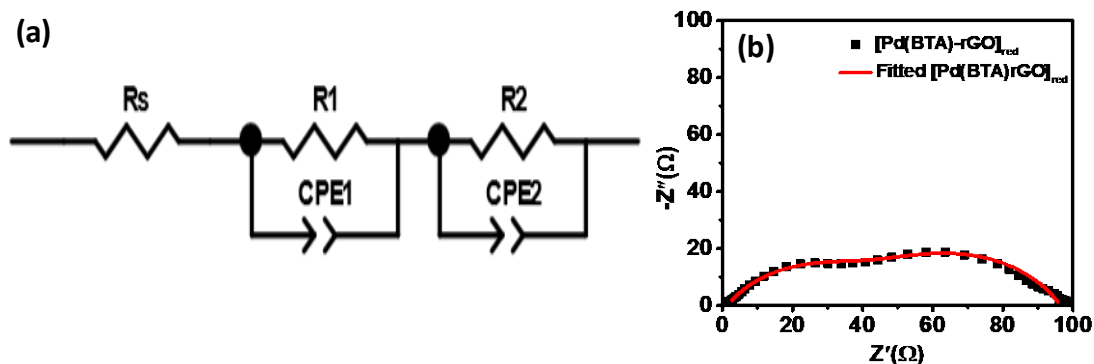
Table S3: Fitted parameters of equivalent circuit model shown in Fig. S15a for **[Pd(BTA)-rGO]red**

Rs (Ω)	R1 (Ω)	CPE1-T (10^{-4}F)	CPE1-P	R2 (Ω)	CPE2-T (10^{-5}F)	CPE2-P	χ^2 (10^{-3})
1.52	52.65	2.7549	0.67	42.18	3.2757	0.64	1.25
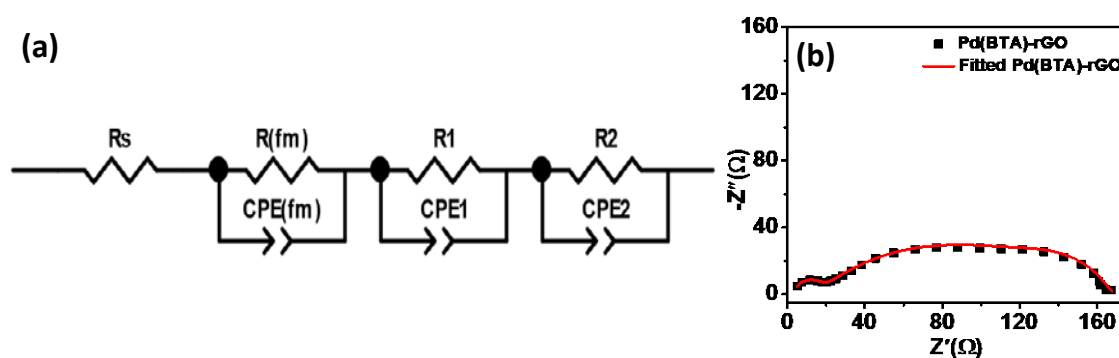
Figure S16. (a) Equivalent circuit model and (b) corresponding fitted diagram of equivalent circuit for **Pd(BTA)-rGO**

Table S4: Fitted parameters of Equivalent circuit model shown in Fig. S16a for **Pd(BTA)-rGO**

Rs (Ω)	R(fm) (Ω)	CPE(fm)-T (10^{-8}F)	CPE(fm)-P	R1 (Ω)	CPE1-T (10^{-4}F)	CPE1-P	R2 (Ω)	CPE2-T (10^{-4}F)	CPE2-P	χ^2 (10^{-4})
2.94	12.18	3.0	0.98	26.1	9.30	0.89	127	1.76	0.52	6.27
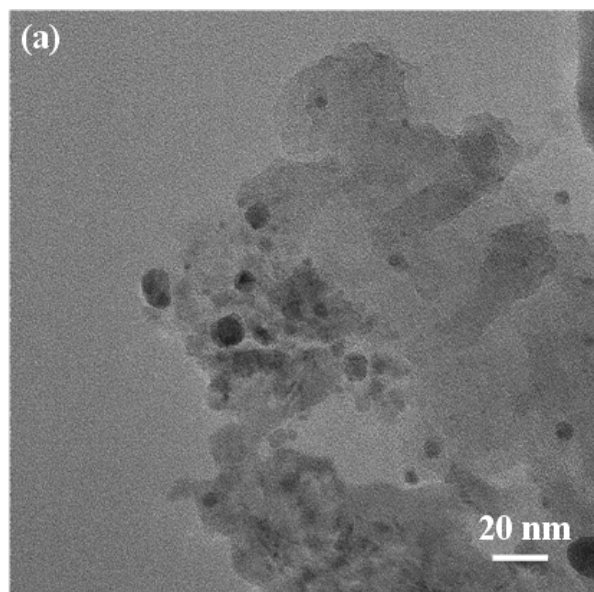
Figure S17. HRTEM image of **[Pd(BTA)-rGO]$_{red}$** after 70 h of HER at a current density of -300 mA/cm^2.

Figure S18. (a) HAADF image of **[Pd(BTA)-rGO]$_{red}$** after cycling at -300 mA/cm^2 for 70 h; (b) & (c) TEM elemental mapping of Pd & Nitrogen..
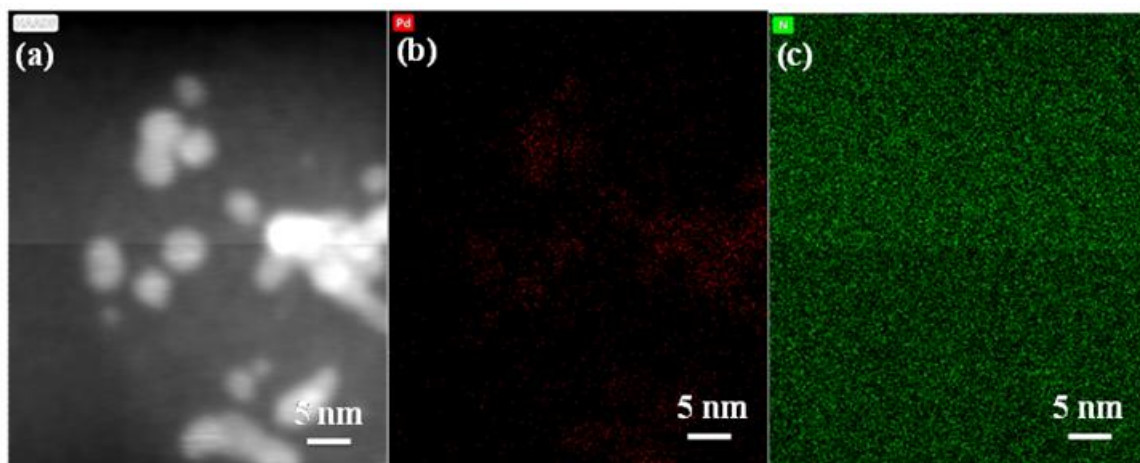
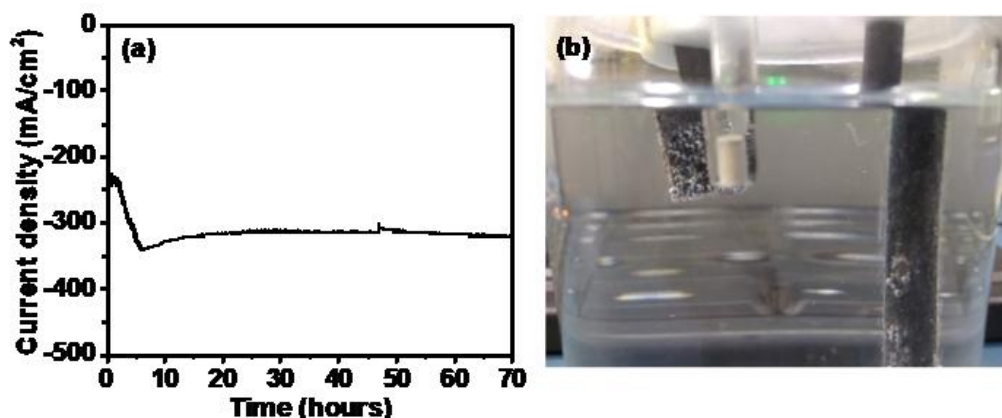**Figure S19.** (a) Chronoamperometric curve of **[Pd(BTA)-rGO]red** using graphite as counter electrode; (b) photograph of cell set-up where the hydrogen evolution is apparent.

Table S5. Comparison of the over potential, Tafel slope and stability of the various Pd-based electrocatalysts reported so far with that of **[Pd(BTA)-rGO]red** realized in the present work.

Sample	Over potential	Tafel slope (mV/dec)	Stability test *via* i-t curve.	Electrolyte	Ref
(PdCo@CN)	-80 mV to attain -10 mA/cm^2	31	~-40 mA/cm^2 for 11 h	0.5 M H$_2$SO$_4$	1
Pd-CNx	-55 mV to attain -10 mA/cm^2	35	-28 mA/ cm^2 for 100 h	0.5 M H$_2$SO$_4$	2
Pd@Zr–AzoBDC MOF	-800 mV to attain -10 mA/cm^2	---	---	0.5 M Na$_2$SO$_4$	3
Pd graphene for HER	----	46	-20 mA/cm^2 for 1500 s	0.5 M H$_2$SO$_4$	4
Pd cube/PEIerGO$_{50:1}$	-100 mV to attain -108 mA/cm^2	34	-150 mA/cm^2 for 72 h	0.5 M H$_2$SO$_4$	5
Pt@Pd NFs/rGO	-56 mV to attain -10 mA/cm^2	39	-15 mA/cm^2 for 10000 s	0.5 M H$_2$SO$_4$	6
Pd$_{3.02}$Te NWs/rGO	-97 mV to attain -10 mA/cm^2	90	-32 mA/cm^2 for 48 h	0.5 M H$_2$SO$_4$	7
PdCu@Pd Nanocube	-10 mV to attain -68 mA/cm^2	35	-220 mA/cm^2 for 48 h	0.5 M H$_2$SO$_4$	8
PdPS reduced graphene oxide composite	-90 mV to attain -10 mA/cm^2	46	----	0.5 M H$_2$SO$_4$	9
Pd nanoparticle assembly	-80 mV to attain -100 mA/cm^2	30	-10 mA/cm^2 for 25000 s	0.5 M H$_2$SO$_4$	10
Pd@MOF-74-Co-3	-106 mV to attain -10 mA/cm^2	57	------	0.5 M H$_2$SO$_4$	11
Co@Pd core-shell particles	-145 mV to attain -10 mA/cm^2	55.7	-10 mA/cm^2 for 10 h	0.5 M H$_2$SO$_4$	12
monoclinic Pd rich PdBi$_2$	-140 mV to attain -20 mA/cm^2	63	------	0.5 M HClO$_4$	13
Pd$_2$Si	-192 mV to attain -10 mA/cm^2	131	------	0.5 M H$_2$SO$_4$	14

Copper benzenehexathiol coordinated polymer Cu[BHT]	-450 mV to attain -10 mA/cm^2	95	-261 mA/cm^2 for 20 hours	0.5 M H$_2$SO$_4$	15
1D helical coordination polymer Zn^{2+}(fcdHp)	-340 mV to attain -10 mA/cm^2	110		0.5 M H$_2$SO$_4$	16
1D helical coordination polymer Co^{2+}(fcdHp)	-450 mV to attain -10 mA/cm^2	120		0.5 M H$_2$SO$_4$	16
[Pd(BTA)-rGO]$_{red}$	-127 mV to attain -10 mA/cm^2	55	-300 mA/cm^2 for 70 h	0.5 M H$_2$SO$_4$	This work

It is immediately apparent that **[Pd(BTA)-rGO]$_{red}$** exhibits a remarkable over potential of -127 mV at -10 mA/cm^2 current density featuring a Tafel slope of 55 mV/dec with high durability of 70 hours at -300 mA/cm^2.

References

1. Chen, J.; Xia, G.; Jiang, P.; Yang, Y.; Li, R.; Shi, R.; Su, J.; Chen, Q., Active and Durable Hydrogen Evolution Reaction Catalyst Derived from Pd-Doped Metal–Organic Frameworks. *ACS Appl. Mater. Interfaces* **2016,** *8* (21), 13378-13383.

2. Bhowmik, T.; Kundu, M. K.; Barman, S., Palladium nanoparticle–graphitic carbon nitride porous synergistic catalyst for hydrogen evolution/oxidation reactions over a broad range of pH and correlation of its catalytic activity with measured hydrogen binding energy. *ACS Catal.* **2016,** *6* (3), 1929-1941.

3. Le, H. V.; Nguyen, Q. T. T.; Nguyen, P. K. T.; Nguyen, H. T., A Composite Based on Pd Nanoparticles Incorporated into a Zirconium-Based Metal–Organic Frameworks Zr–AzoBDC and Its Electrocatalytic Activity for Hydrogen Evolution Reaction. *J. Electron. Mater.* **2018,** *47* (11), 6918-6922.

4. Ghasemi, S.; Hosseini, S. R.; Nabipour, S.; Asen, P., Palladium nanoparticles supported on graphene as an efficient electrocatalyst for hydrogen evolution reaction. *Int. J. Hydrogen Energy* **2015,** *40* (46), 16184-16191.

5. Li, J.; Zhou, P.; Li, F.; Ma, J.; Liu, Y.; Zhang, X.; Huo, H.; Jin, J.; Ma, J., Shape-controlled synthesis of Pd polyhedron supported on polyethyleneimine-reduced graphene oxide for enhancing the efficiency of hydrogen evolution reaction. *J. Power Sources* **2016,** *302*, 343-351.

6. Lin, X.-X.; Wang, A.-J.; Fang, K.-M.; Yuan, J.; Feng, J.-J., One-pot seedless aqueous synthesis of reduced graphene oxide (rGO)-supported core–shell Pt@ Pd nanoflowers as advanced catalysts for oxygen reduction and hydrogen evolution. *ACS Sustainable Chem. Eng.* **2017,** *5* (10), 8675-8683.

7. Jiao, L.; Li, F.; Li, X.; Ren, R.; Li, J.; Zhou, X.; Jin, J.; Li, R., Ultrathin PdTe nanowires anchoring reduced graphene oxide cathodes for efficient hydrogen evolution reaction. *Nanoscale* **2015,** *7* (44), 18441-18445.

8. Li, J.; Li, F.; Guo, S.-X.; Zhang, J.; Ma, J., PdCu@ Pd nanocube with Pt-like activity for hydrogen evolution reaction. *ACS Appl. Mater. Interfaces* **2017,** *9* (9), 8151-8160.

9. Sarkar, S.; Sampath, S., Equiatomic ternary chalcogenide: PdPS and its reduced graphene oxide composite for efficient electrocatalytic hydrogen evolution. *Chem. Commun.* **2014,** *50* (55), 7359-7362.

10. Liu, S.; Mu, X.; Duan, H.; Chen, C.; Zhang, H., Pd nanoparticle assemblies as efficient catalysts for the hydrogen evolution and oxygen reduction reactions. *Eur. J. Inorg. Chem.* **2017,** *2017* (3), 535-539.

11. Zheng, F.; Zhang, C.; Gao, X.; Du, C.; Zhuang, Z.; Chen, W., Immobilizing Pd nanoclusters into electronically conductive metal-organic frameworks as Bi-functional electrocatalysts for hydrogen evolution and oxygen reduction reactions. Electrochim. Acta **2019**.

12. Yang, H.; Tang, Z.; Wang, K.; Wu, W.; Chen, Y.; Ding, Z.; Liu, Z.; Chen, S., Co@ Pd core-shell nanoparticles embedded in nitrogen-doped porous carbon as dual functional electrocatalysts for both oxygen reduction and hydrogen evolution reactions. *J. Colloid Interface Sci.* **2018,** *528*, 18-26.

13. Sarkar, S.; Subbarao, U.; Peter, S. C., Evolution of dealloyed PdBi 2 nanoparticles as electrocatalysts with enhanced activity and remarkable durability in hydrogen evolution reactions. *J. Mater. Chem. A* **2017,** *5* (30), 15950-15960.

14. McEnaney, J. M.; Schaak, R. E., Solution synthesis of metal silicide nanoparticles. *Inorg. Chem.* **2014,** *54* (3), 707-709.

15. Huang, X.; Yao, H.; Cui, Y.; Hao, W.; Zhu, J.; Xu, W.; Zhu, D., Conductive copper benzenehexathiol coordination polymer as a hydrogen evolution catalyst. *ACS Appl. Mater. Interfaces* **2017,** *9* (46), 40752-40759.

16. Shekurov, R.; Khrizanforova, V.; Gilmanova, L.; Khrizanforov, M.; Miluykov, V.; Kataeva, O.; Yamaleeva, Z.; Burganov, T.; Gerasimova, T.; Khamatgalimov, A., Zn and Co redox active coordination polymers as efficient electrocatalysts. *Dalton Trans.* **2019,** *48* (11), 3601-3609.